A statistical investigation of particle crushing in sand

G. Marketos & M.D. Bolton
Centre of Geotechnical Process and Construction Modelling, Cambridge University Engineering Department, Cambridge, U K

International Symposium on Geomechanics and Geotechnics of Particulate Behaviour, Yamaguchi, September 2006, 247-252.

ABSTRACT: The deformation of a volume of sand comes about from particle rearrangement to new positions, and from particle crushing at larger stresses. It is desirable to be able to quantify the level of crushing inside a sand, as this affects the grain size distribution of the sample, which is directly linked to its permeability. In addition, under certain conditions, which need to be clarified, the crushing of one particle may lead to the crushing of a near neighbour, ultimately leading to the formation of a propagating compaction band. An attempt will be presented here to understand and predict the extent of crushing using a statistical analysis based on the results of discrete element simulations. The distributions of intergranular contact forces inside a DEM model of a sand will be coupled with an idealised distribution of crushing strengths of the sand grains. These will be combined to obtain the probabilities of crushing of grains within a stressed assembly. It is anticipated that DEM analyses and statistical reasoning may permit engineers to use grain-scale tests to predict the extent of crushing in a sample, and ultimately discriminate between cases of homogeneous crushing throughout a volume of sand and localised crushing in a compaction band.

1 INTRODUCTION

The significance of particle crushing in the stress-strain behaviour of sands has long been recognised. McDowell & Bolton (1998) have related successfully the normal compression line of sand to fractal crushing of particles, while Cheng et al (2004) have identified the yield surface of a sand as a contour of crushing.

In addition, as particle crushing changes the grain-size distribution of a sample it will directly affect its permeability. One should distinguish two cases here: homogeneously distributed crushing which is the norm, and localised crushing (e.g. Di-Giovanni et al. 2001). Crushing localisation forms in thin tabular zones of large extent that are called compaction bands. Permeability inside a band is decreased by an order of magnitude (Mollema & Antonellini 1996) severely affecting the flow field inside a sample by creating preferential flow paths. It should be noted that crushing localisation has been reported in sandstone only, but Marketos & Bolton (2005) report computer simulations that suggest that it could also occur in sand.

It is therefore advantageous to be able to quantify the extent of crushing in a soil sample and predict whether it will be localised. Most approaches are based on continuum mechanics which is presently incapable of describing this information. A tool based on micromechanics needs to be developed as this will relate crushing to relevant grain properties. Nakata et al (1999) have attempted to relate the extent of crushing observed experimentally to the crushing strength of particles. However the great practical difficulties of doing so in an experiment meant that they had to resort to using a rather simplified approach. A small number of particles was chosen at random and the damage to them was tracked, by exhumation and photography. The force distribution was not known, so the simplifying assumption of equal force causing crushing on all particles was adopted. An alternative method of investigation can be based on Discrete Element Modeling. This has the advantage of easy access to the multitude of data involved and can yield information on micromechanical parameters of interest (such as the internal grain-force distribution) which are otherwise inaccessible.

We will therefore use a discrete element method to simulate crushing in a sand element under one-dimensional compression. Another simulation will be used to obtain the distribution of inter-particle contact forces. These will be combined to confirm our hypothesis that a statistical analysis of particle crushing can be successful in predicting the extent of crushing. Insight gained here will allow the development of further statistical tools that are needed to understand and describe crushing localisation.

2 DISCRETE ELEMENT METHOD

Two different discrete element simulations were performed. One was performed on a sample where crushing was suppressed and the only possible micromechanism was particle rearrangement. This was carried out in order to calculate the force distribution inside a sand, which would later be used as an input to the statistical analysis.

The second simulation was performed on the same sample, this time allowing particle crushing. Data regarding the extent of crushing were recorded. These simulations were performed using the code PFC^{3D} which is commercially available by Itasca Inc. A concise description of this code can be found in the PFC^{3D} manual (Itasca Inc. 2003).

The sample used was cuboidal (porosity 44.8%, dimensions 6 cm x 6 cm x 7.2 cm). It consisted of 8943 spherical particles of radii uniformly distributed between 1 and 2 mm. It was prepared by a simulated 'numerical dry pluviation' and was bounded by frictionless walls on all sides. No gravity forces were included and a soft contact approach was used. The side walls were kept stationary while a constant axial shortening rate of 0.1 m/s was applied. The micromechanical parameters used in the simulations can be found in Table 1. It should be noted that the values for stiffness are of the order of magnitude inferred from single crushing tests on quartz particles reported by Nakata et al. (1999). All the data presented below were recovered from an inspection volume that excluded the region lying within three particle diameters of the top and bottom boundary, where the non-random fabric might lead to preferential crushing.

Table 1: Micromechanical parameters used for the simulation

Parameter	Numerical Value
normal and shear stiffness of balls	4 x 10^6 N/m
normal and shear stiffness of walls	4 x 10^6 N/m
particle friction coefficient, μ_b	0.5
wall friction coefficient, μ_w	0.0
density of spheres	2650 kg/m^3
coefficient of local damping	0.7
sample shortening rate	0.1 m/s

2.1 *Simulation with no crushing*

The normal contact force distribution inside the sample was followed throughout the simulation. The distribution was found to be approximately the same for different stress levels when contact force was non-dimensionalised in terms of its the mean value. This is plotted in Figure 1. It should be noted that this plot is a probability density function, which means that the probability of finding a normalised force with magnitude between x and x+Δx is given by the area under the curve. It was found that this curve has an exponential tail for large forces and can

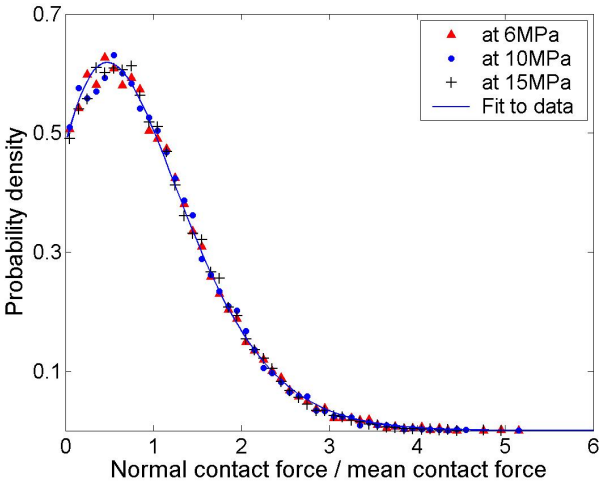

Figure 1: A plot of the probability density function of normal contact force over mean contact force for three different stress levels.

be fitted by the curve $(x+\Delta)^B \cdot e^{-\Gamma x+E}$, where B, Γ, Δ, and E are constants. This force distribution is similar to those previously reported in the literature (see e.g. Radjai et al. 1996 or Thornton 1997).

In our case, however, it is not the distribution of all the contact forces that is important. We will be assuming that it is the maximum normal force on a particle that causes crushing, irrespective of what the other contact forces are. We are then more interested in the distribution of the maximum force exerted on particles. This is plotted in Figure 2 on normal, and in Figure 3 on semi-logarithmic axes. Again it is relatively independent of the stress level when plotted against non-dimensionalised force. One should note that the force axis of Figures 1 and 2 is not the same, as the mean normal force based on all contacts and the mean maximum normal force on all particles are clearly not the same.

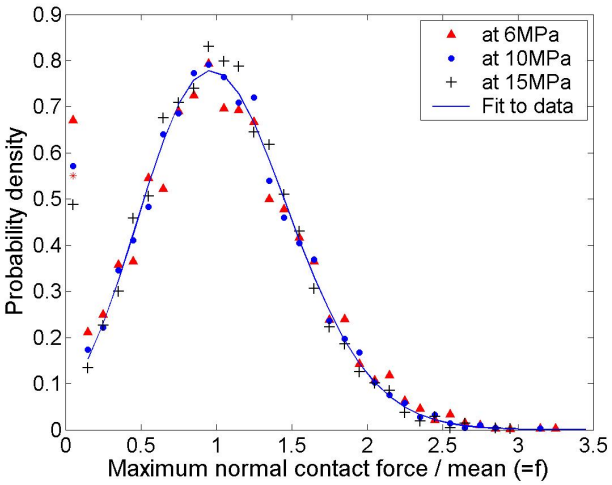

Figure 2: A plot of the probability density function of the maximum normal contact force on a particle (as non-dimensionalised by the mean maximum normal force) for three different stress levels.

The distribution of Figure 2 was fitted by the function

$$g(f) = (f + a)^b e^{-cf - d} \qquad a = 2.6, b = 53, c = 15, d = 54 \tag{1}$$

where f is the ratio of the maximum normal contact force on a given particle to its mean value for all particles. As seen in Figure 3, for forces larger than 2 F_{mean} the distribution can be approximated by an exponential decay of the form $\alpha e^{-\beta f}$, with α=247 and β=3.77. This exponential fit is included in Figure 3.

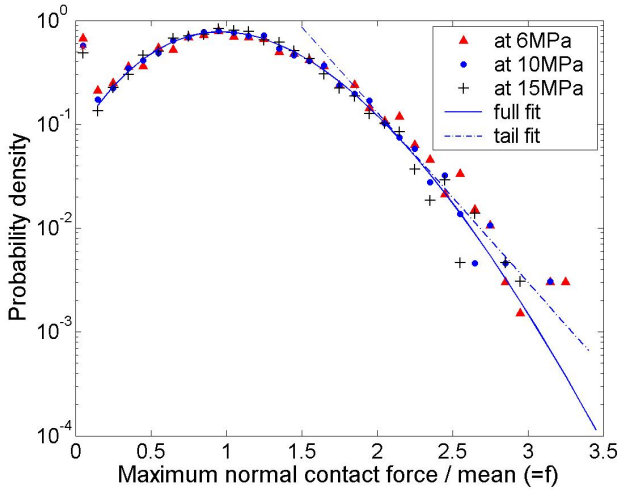

Figure 3: The same plot as in Figure 2 but this time plotted on semi-logarithmic axes.

2.2 *Crushing simulation*

Crushing events were simulated as follows. A characteristic strength parameter was assigned to each particle. A particle was then completely removed, so as to simulate crushing, when the maximum normal contact force acting on it exceeded its characteristic strength. This represents small fragments, produced by crushing, falling into the pore space and losing their force-carrying capacity. A very similar method of representing crushing by particle removal has been used by Couroyer et al. (2000) and was seen to yield good results.

The strength parameter was randomly assigned to each particle and its overall distribution was chosen to be approximately of the form of Equation 2:

$$h(\Phi) = 0.0395/\sqrt{\Phi}, \Phi_{max} = 640N, \Phi_{min} = 160N \tag{2}$$

where Φ is the characteristic strength parameter in Newtons. A plot of the distribution of particle strengths is shown in Figure 4, along with the function of Equation 2.

One should note that this distribution was chosen arbitrarily and does not describe any physical situation. It is used as an input to the simulation. The purpose of this work is to set up and validate the statistical method outlined here, and this completely arbitrary function is suitable for our purposes. Any other distribution can be chosen instead and some (e.g. uniform, Weibull, etc), might be thought more realistic. Note that equation 2 is consistent with a characteristic breaking stress (force divided by square diameter) for a particle in the range of 10-160 MPa.

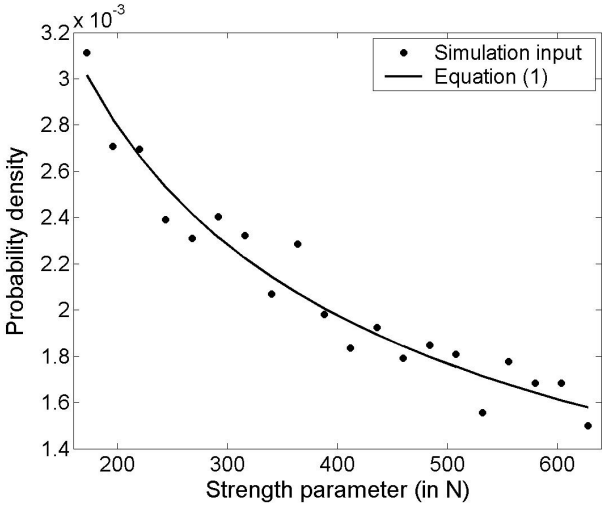

Figure 4: A plot of the distribution of strength parameters as used in the simulation and as approximated by Equation 2.

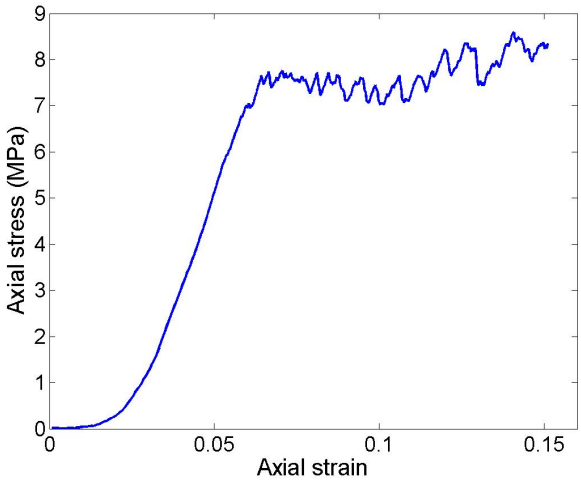

Figure 5: The axial stress plotted versus the axial strain for the crushing simulations.

These simulations yielded the stress-strain curve of Figure 5. The initial response up to 0.05 strain is only due to particle rearrangement and with slipping at contacts initiated by elastic shortening at the contacts. Crushing of particles is initiated at a strain of 0.053. As more particles crush the stiffness of the sample decreases and finally a crushing plateau is

reached beyond a strain of 0.065. One should note that the stress-strain curve exhibits instabilities, which for similar simulations have been shown to correspond to localised crushing (Marketos & Bolton 2005). Various other micromechanical parameters were traced throughout this simulation and were used to check the validity of the proposed statistical analysis outlined below.

3 STATISTICAL ANALYSIS

The probability of two events occurring is given by the product of the two individual probabilities, if we can assume that these two events are independent. In the case discussed here we have randomly chosen the strength of each particle from the distribution of Equation 2. We can therefore be certain that it will be independent of the force on it. This however might not be the case if the strength were a function of particle size, as we have seen that large forces tend to concentrate on larger particles.

From the above we can say that the probability of crushing for a particle with a given strength will be just the probability that the maximum normal force on it exceeds its strength. This is in turn given by the integral of Equation 3, or the relevant area under the probability density curve of Figure 2.

$$p = \int_{\varphi}^{+\infty} g(f)df \tag{3}$$

where p is the probability of crushing of a specific particle at a given macroscopic stress, φ and f are this particle's strength and maximum particle force respectively each non-dimensionalised by the mean of the maximum force on all particles, and g is the probability density function for maximum particle normal force as plotted in Figure 2.

One can further extend this argument to the full case, where the strength of the particles itself follows a certain distribution. Now there is also a probability associated with the strength of the particle having a certain value (as plotted in Fig. 4). The probability of a crushing event will be given by the summation of the products of the probabilities of the two independent events: the probability that the strength has a value Φ, and that the grain-force is larger than Φ. This should be done for all possible values of particle strength. In the limit of continuous distributions for both the above quantities the summation becomes an integral and the probability of a crushing event is given by Equation 4. This is sometimes termed the convolution integral.

$$P = \int_{Strength_{\min}}^{Strength_{\max}} p(Strength = \Phi)\, p(Force > \Phi) d\Phi \tag{4}$$

In our case substituting the relevant probability distribution functions into Equation 4 we get Equation 5. One should note that this step involves a change of variable inside the integral calculating the probability of force exceeding Φ, as the function g is in terms of normalized force (f), while Φ is a force in Newtons. This is how the mean force term ($\overline{F}$) comes into the calculation.

$$P = \int_{\Phi_{\min}}^{\Phi_{\max}} h(\Phi) \left(\int_{\Phi}^{+\infty} g(F/\overline{F}) dF/\overline{F} \right) d\Phi = \tag{5}$$

$$= \int_{160}^{640} \frac{0.0395}{\sqrt{\Phi}} \left(\int_{\Phi}^{+\infty} (F/\overline{F} + 2.6)^{53} e^{-15F/\overline{F} - 54} dF/\overline{F} \right) d\Phi \tag{6}$$

Here P is the probability of crush of a particle, Φ and F are this particle's strength and maximum particle force respectively, $\overline{F}$ is the mean of the maximum forces on all particles, g is the probability density function for maximum particle force as plotted in Figure 2 and h is the probability density function for particle strength as plotted in Figure 4.

One can easily implement the integral of Equation 6 numerically to get a prediction of the crushing probability for one grain. This has been plotted in Figure 6. It should be noted that Equation 6 implies that P is only a function of the mean maximum force on particles. If a relation between stress and crushing probability is needed relations between stress and mean force would need to be assumed. Such relations would be only a function of the grain structure of the sand meaning that two sands with the same grain size distribution but different structure would exhibit different stress-strain curves.

One should also note that we could use the exponential tail approximation to the force probability density function. This would allow the analytical calculation of Equation 4 and would provide an approximation to the probability of one crush (Eq. 7).

$$P = \int_{160}^{640} \frac{0.0395}{\sqrt{\Phi}} \left(1/\overline{F} \int_{\Phi}^{+\infty} 247 e^{-3.77F/\overline{F}} dF \right) d\Phi \tag{7}$$

Figure 6 also contains a plot of the crushing probability versus mean force as observed in the crushing simulation outlined above. This probability was calculated as the ratio of the cumulative count of particles that have crushed at each instant over the total number of particles in the simulation initially. One can observe that the curves in Figure 6 agree very well with each other initially and up to a mean maximum particle normal contact force of 80 Newtons.

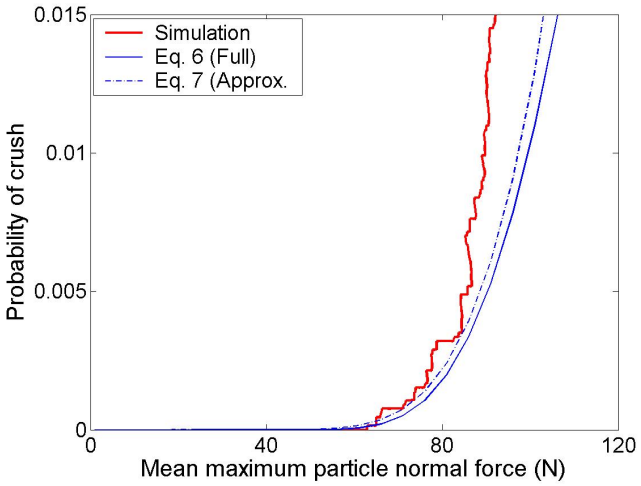

Figure 6: A plot of the probability of one crush versus mean maximum particle force as given by Equations 6 (the full convolution) and 7 (using the exponential tail approximation). Note that these correspond to the smooth curves in this plot. The results of the crushing simulations are also plotted for comparison.

4 DISCUSSION

One should note that the calculation of the probability of crushing using Equation 4 is relevant to cases where all the crushes happen simultaneously. This is mostly applicable to the case where the sample is stressed rapidly. In the crushing simulation presented here particles are crushed sequentially so that at every instant the probability based on the cumulative crush count is larger than the probability predicted by Equation 4.

One should note that the prediction for the initiation of crushing is very accurate and that the results are in very good agreement up to a value of mean force of 90N, or a probability of 0.004. This is no coincidence. In this initial region we can assume that crushing events are completely independent of each other as the stress-carrying network inside the sample has not been significantly disturbed.

If however one wanted to predict more accurately the extent of crushing after this initial region a more complicated approach would be needed. This would involve calculating the variation in the force network after an initial crushing event and would be aiming to calculate the conditional probability of a second crush occurring given that a particle has already crushed.

Statistical approaches based on the calculation of the perturbation of the force network due to an initial crush might hold the key to understanding the formation of crushing localisation. This is the main motivation behind the present simplified statistical study. Compaction bands induced during the drilling of oil wells have been implicated in wellbore instability mechanisms (Haimson 2001), as well as in the concern of reservoir engineers to predict the extent of sand fines production. The dual concerns of particle crushing and crushing localisation seem to demand an understanding of material behaviour from the particulate and statistical standpoint taken here.

5 CONCLUSION

The statistical method proposed here has been shown to produce results in good agreement to the ones observed in discrete element simulations of crushing. This method has been seen to predict the onset of crushing and allows one to quantify the level of crushing. We have seen that the simplifying approximation of an exponential decay of contact force introduces a very small error in the calculation. Even though the method has been compared with fictitious results from a simulation one would expect that it should work for sand samples as well. The following experimental sequence might therefore be imagined.

A series of single-particle crushing tests is conducted, large enough to obtain an accurate estimate of the probability density of particle strength. The probability density function of particle force is then estimated based on a computer simulation of a sand sample with similar grain size distribution. The two functions are combined using Equation 4 to yield the probability of crush of one particle.

To sum up, the results presented here have demonstrated that a statistical treatment of sand is valid and might prove advantageous in the analysis of soil crushing. It is thought that such methods might hold the key to understanding when and why localisation might occur. Furthermore they might allow one to relate aspects of soil behaviour to well-defined micromechanical parameters that have a physical meaning, a direction in which classical approaches based on continuum mechanics have failed.

ACKNOWLEDGEMENTS

The authors would like to thank the A.G. Leventis Foundation and the A.S. Onassis Foundation for their generous financial support.

REFERENCES

Cheng, Y.P., Bolton, M.D. & Nakata, Y. 2004. Crushing and plastic deformation of soils simulated using DEM, *Geotechnique* 54 (2): 131-141

Couroyer, C., Ning Z. & Ghadiri M. 2000. Distinct element analysis of bulk crushing: effect of particle properties and loading rate, *Powder Technology,* 109: 241-254

DiGiovanni, A.A., Fredrich, J.T., Holcomb, D.J. & Olsson, W.A. 2001. Microscale damage evolution in compacting sandstone. In G. Couples, P. Meredith & I. Main (eds), *Fracture, Damage and Related Deformation Features*. Geological Society of London Special Publication

Haimson, B. 2001. Fracture-like Borehole Breakouts in High-Porosity Sandstone: Are they Caused by Compaction Bands?, *Physics and Chemistry of the Earth, Part A,* 26 (1-2): 15-20

Itasca Consulting Group, Inc. 2003. *PFC^{3D}: Particle Flow Code in 3 Dimensions, Version 3.0*, Minneapolis, U.S.A.

McDowell, G.R. & Bolton, M.D. 1998. On the micromechanics of crushable aggregates, *Geotechnique*, 48 (5): 667-679.

Marketos, G. & Bolton, M.D. 2005. Compaction bands as observed in DEM simulations. In R. Garcia-Rojo, H.J. Herrmann & S. McNamara (eds), *Powders and Grains, Proc. Int. conf. Stuttgart, July 2005*. 2: 1405-1409

Mollema, P.N. & Antonellini, M.A. 1996. Compaction bands: a structural analog for anti-mode I cracks in Aeolian sandstone. *Tectonophysics*, 267: 209-228

Nakata, Y., Hyde, A.F.L., Hyodo, M. & Murata, H. 1999. A probabilistic approach to sand particle crushing in the triaxial test, *Geotechnique*, 49 (5): 567-583

Radjai, F., Jean, M., Moreau, J.-J. & Roux, S. 1996. Force distributions in dense two-dimensional granular systems, *Physical Review Letters*, 77 (2): 274-277

Thornton, C. 1997. Force transmission in granular media, *KONA*, 15: 81-90